Water Resources Research

RESEARCH ARTICLE
10.1029/2019WR024816

Key Points:
- Fraction recharge in groundwater is reconstructed from end-member modeling via Monte Carlo simulations of constrained source distributions
- Groundwater from standing water sources has dissolved arsenic concentrations proportional to dissolved organic carbon concentrations
- Groundwater derived from riverine sources contains high arsenic but lower and uncorrelated dissolved organic carbon concentrations

Supporting Information:
- Supporting Information S1
- Table S1
- Movie S1

Correspondence to:
B. C. Bostick,
bostick@ldeo.columbia.edu

Citation:
Nghiem, A. A., Stahl, M. O., Mailloux, B. J., Mai, T. T., Trang, P. T., Viet, P. H., et al. (2019). Quantifying riverine recharge impacts on redox conditions and arsenic release in groundwater aquifers along the Red River, Vietnam. *Water Resources Research*, *55*, 6712–6728. https://doi.org/10.1029/2019WR024816

Received 21 JAN 2019
Accepted 18 JUL 2019
Accepted article online 29 JUL 2019
Published online 10 AUG 2019

Quantifying Riverine Recharge Impacts on Redox Conditions and Arsenic Release in Groundwater Aquifers Along the Red River, Vietnam

Athena A. Nghiem[1,2], Mason O. Stahl[3], Brian J. Mailloux[4], Tran Thi Mai[5], Pham Thi Trang[5], Pham Hung Viet[5], Charles F. Harvey[6], Alexander van Geen[2], and Benjamin C. Bostick[2]

[1]Department of Earth and Environmental Sciences, Columbia University, New York, NY, USA, [2]Lamont-Doherty Earth Observatory, Columbia University, Palisades, NY, USA, [3]Department of Geology, Union College, Schenectady, NY, USA, [4]Department of Environmental Sciences, Barnard College, New York, NY, USA, [5]Research Centre for Environmental Technology and Sustainable Development, Hanoi University of Science and Technology, Vietnam National University, Hanoi, Vietnam, [6]Department of Civil and Environmental Engineering, Massachusetts Institute of Technology, Cambridge, MA, USA

Abstract Widespread contamination of groundwater with geogenic arsenic is attributed to microbial dissolution of arsenic-bearing iron (oxyhydr)oxides minerals coupled to the oxidation of organic carbon. The recharge sources to an aquifer can influence groundwater arsenic concentrations by transport of dissolved arsenic or reactive constituents that affect arsenic mobilization. To understand how different recharge sources affect arsenic contamination—in particular through their influence on organic carbon and sulfate cycling—we delineated and quantified recharge sources in the arsenic affected region around Hanoi, Vietnam. We constrained potential end-member compositions and employed a novel end-member mixing model using an ensemble approach to apportion recharge sources. Groundwater arsenic and dissolved organic carbon concentrations are controlled by the dominant source of recharge. High arsenic concentrations are prevalent regardless of high dissolved organic carbon or ammonium levels, indicative of organic matter decomposition, where the dominant recharge source is riverine. In contrast, high dissolved organic carbon and significant organic matter decomposition are required to generate elevated groundwater arsenic where recharge is largely nonriverine. These findings suggest that in areas of riverine recharge, arsenic may be efficiently mobilized from reactive surficial environments and carried from river-aquifer interfaces into groundwater. In groundwaters derived from nonriverine recharge areas, significantly more organic carbon mineralization is required to obtain equivalent levels of arsenic mobilization within inland sediments. This method can be broadly applied to examine the connection between hydrology, geochemistry and groundwater quality.

1. Introduction

Geogenic arsenic contamination poses an immense public health threat, especially to those in South and Southeast Asia, who rely on groundwater for drinking water and irrigation (Fendorf et al., 2010). In most of South and Southeast Asia, arsenic is released to the groundwater by microbial reduction of arsenic-bearing iron (Fe) (oxyhydr)oxides in anoxic environments. The dissolution of Fe (III) minerals is driven by microbial oxidation of organic carbon (OC) to CO_2 coupled to the reduction of Fe (III) (Oremland & Stolz, 2005). This reactive OC may come from internal sources such as either older OC originally deposited with sediments and typically assumed to be more recalcitrant or younger external sources. These external sources include surficial sediments generating dissolved OC (DOC) or anthropogenic surface-derived sources, such as wastewater. However, the significance of each of these sources to the reactive OC pool that enhances Fe reduction and arsenic release in sediments remains highly debated (Dowling et al., 2002; Mailloux et al., 2013; Postma et al., 2012; Rowland et al., 2006). Sulfur cycling also can potentially affect arsenic concentrations by producing insoluble arsenic sulfides (Saalfield & Bostick, 2009; Sun, Quicksall, et al., 2016). However, sulfide, the product of sulfate reduction, can also indirectly solubilize arsenic because it causes Fe (III) reduction (Burton et al., 2014; Saalfield & Bostick, 2009) and complexes dissolved arsenic (Bostick et al., 2005; Suess & Planer-Friedrich, 2012).

Hydrologic conditions regulate the source and location of recharge and the evolution of groundwater chemical composition during flow. Sustaining high-quality (low arsenic) water resources over the long-term thus involves an understanding the hydrological context of relevant biogeochemical processes. Recharge sources can carry distinct compositions of dissolved loads of geochemically active constituents like arsenic, DOC, and sulfate that affect arsenic retention in the solid phase. For example, if OC is primarily young DOC, then advected OC from river or surface water is likely reactive and can exacerbate arsenic contamination (Mailloux et al., 2013). River sediments can also host reactive OC that drives arsenic mobilization during riverine recharge; the recharge water itself, however, may not maintain high DOC as it is consumed before advection into the aquifer (Postma et al., 2010, 2017; Stahl et al., 2016). Perturbations in regional hydrology associated with urban water use under anthropogenic pumping in the Red River Delta near Hanoi, Vietnam, has increased riverine recharge and reversed groundwater flow and resulted in the lateral contamination of previously low arsenic aquifers—raising concerns about the vulnerability and sustainability of these aquifer systems (Berg et al., 2008; van Geen et al., 2013).

In this work, we bridge the gap between local-scale investigations of heterogeneity and the larger Red River Delta (Kuroda, Hayashi, Funabiki, et al., 2017; Richards et al., 2018; Winkel et al., 2011). We focus on a regional-scale study of hydrology and geochemistry along the Red River near Hanoi. While physical measurements of groundwater heads are valuable in determining flow patterns, they only provide a snapshot of current conditions, and in many situations it is difficult or impractical to employ these data to identify groundwater recharge sources. In this area, the spatially complex and transient nature of the regional hydrology coupled with groundwater ages that exceed available head data collected over much shorter time scales limits the applicability of using head data to determine recharge source. Thus, we rely on stable water isotopes and conservative ion concentrations to give insight and information into physical hydrology of our studied system in our end-member mixing analysis to determine fraction recharge from different sources.

Usually, recharge source distributions are calculated from specific end-member composition for each recharge source (Christophersen & Hooper, 1992; Clark & Fritz, 1997; Correa et al., 2019). Often, one of the key challenges in resolving the flow path to aquifers is that the flow path and hydraulic gradient of all the wells at all times is unknown. Here, however, we do not require the knowledge of the flow path or direction or a single source composition. Our method improves traditional methods of end-member mixing analysis by using hydrogeological data to define a range of possible source composition and performs ensemble modeling and Monte Carlo simulation of source distributions that give the most probable fraction recharge for a particular recharge source. The Red River is a large fluvial system with uniquely isotopically light headwater that differs considerably from local precipitation, making it ideal to model with our approach.

The unique ability to reconstruct recharge source fractions allows us to delineate novel relationships with geochemistry that we would not discern otherwise, especially for large data sets. This offers a novel approach generalizable to determining groundwater recharge fraction in hydraulic regimes with limited hydrograph information based primarily on conditions of flow systems. From relationships and analysis of variance against modeled fraction recharge, we examine how differences in the hydrology and recharge sources affect arsenic concentrations, and how human perturbations to the aquifer system caused by urban pumping and irrigation are affecting recharge source and groundwater quality. Differentiating these recharge sources could be important in characterizing aquifer redox status, as recharge from both pond and rivers sources can both enhance arsenic release (Kuroda, Hayashi, Do, et al., 2017; Majumder et al., 2016; Stahl et al., 2016; van Geen et al., 2013; Xie et al., 2008). We expect that groundwater contains a large fraction of riverine recharge that results in different redox processes contributing varying amounts of DOC and a heterogeneous signature in sulfate that ultimately affects water quality.

2. Methods

2.1. Field Site

In the Red River Delta, groundwater samples were collected from a sampling survey of domestic wells conducted in collaboration with Hanoi University of Science Research Centre for Environmental Technology and Sustainable Development in December 2013 to May 2014 for a total of 150 groundwater samples with a sample density of approximately one sample per square kilometer. Additional river, pond and groundwater samples were collected from 2013 to 2017, including from well transects drilled on the west bank of the Red

River in the village of Van Phuc. In 2016–2017, other well samples were also taken from orthogonal transects just north of Van Phuc: in the village of Yen My near the Hanoi cone of depression and on the east bank of the Red River in the village of Van Duc, for a total of 183 groundwater samples with an average depth of 36.9 m and spread of 7–80 m with the interquartile range falling between 27 and 45 m. Each well was sampled only once in this study. River water from the Red River was also sampled during this time period in 2016–2017.

2.2. Water Sampling

For each groundwater sample, measurements of field parameters (pH, specific conductivity, and redox potential) were collected with calibrated field probes (Hach portable multimeter HQ30d and HQ40d with Intellical pH probe PHC20 and Intellical conductivity probe CDC401, Accumet AP72 meter with Fisherbrand ORP probe model 13-620-81) and GPS measurements recorded. Water samples, collected for stable water isotope and anion analyses, were filtered through 0.2-μm Supor hydrophilic polyethersulfone (PES) filters into 20-ml *high-density polyethylene* scintillation vials. To minimize evaporation effects, samples were filled with no remaining headspace, sealed with Parafilm, and stored in the dark for shipment to New York before processing. For trace metal analyses, water samples were filtered through 0.2-μm Supor (PES) filters into 20-ml *high-density polyethylene* scintillation vials and acidified with 1% HNO_3. Samples for DOC analysis were filtered through 0.2-μm Supor (PES) filters into 25-ml glass vials that were baked overnight at 450 °C and acidified with 1% HCl. Rain, river, and surface waters were also sampled using the same protocol.

2.3. Water Composition

Stable water isotope analysis was performed on the filtered, unacidified water samples at the Stable Isotope Ratios for Environmental Research lab at the University of Utah for analyses of δ^2H and $\delta^{18}O$ values. Raw instrumental data were corrected based on two primary laboratory reference materials for a two-point normalization method with an additional secondary reference material. The reference materials were calibrated against National Institute of Standards and Technology (NIST)/IAEA certified references. Values are reported in δ notation ($\delta = (R_{sample}/R_{standard} - 1) * 1{,}000$) with units of per mille (‰), relative to Vienna Standard Mean Ocean Water scale. The average precision for δ^2H was 1.1‰ and $\delta^{18}O$ was 0.2‰ for the replicated analyses of the standards across the run. Chloride (Cl^-), bromide (Br^-), and sulfate (SO_4^{2-}) were measured using a Dionex ICS-2000 ion chromatograph equipped with an IonPac AS18 analytical column (Sun, Chillrud, Mailloux, & Bostick, 2016). This method had a detection limit of 30–50 μg/L for halides. The dissolved concentrations of arsenic, iron, sulfur, bromine, and other relevant trace elements were measured via an Element 2 inductively coupled plasma mass spectrometer using germanium as an internal standard to correct for instrument drift (van Geen et al., 2013; Sun, Quicksall, et al., 2016). Accuracy and precision were tested with an internal lab standard and two NIST standards, NIST1640a and NIST1643f, with reliability within <5% for all elements, and the blank detection limits (determined as 3 times average standard deviation of blanks, accounting for all dilutions) were 0.2 μg/L for arsenic, <1 μg/L for Fe, ~14 μg/L for S, and 0.3 μg/L for Br. DOC was measured using the nonpurgable OC method on Shimadzu total organic carbon (V) analyzer using a standard of K phthalate and average precision of 0.05 mg C/L (Sun, Chillrud, Mailloux, Stute, et al., 2016; van Geen et al., 2013).

2.4. Water Level Measurements

From August 2016 to October 2017, the stage of the Red River was measured every 5 min using a pressure transducer (Solinst Levelogger) deployed in the river. These data were barometrically corrected and referenced according to mean sea level elevation (absolute elevation). A well elevation survey was collected using a combination of high-resolution total station GPS methods and traditional surveying compared to a benchmark by the Hanoi University of Science Department of Geography during April 2017. Relative elevations of selected surface well pairs were confirmed with a water leveling tube. Relative error estimates based on loop closure are within 1–2 cm. Absolute elevation of the river was determined with a manual survey measuring the relative elevation of the river surface to a known elevation point at a specific point in time. Here, the water year 2016–2017 (as defined by the U.S. Geological Survey) is used as a typical indicator of monsoonal influence on Red River water levels, aligning with the groundwater samples collected that year. Although water isotopic composition was also sampled at sites in other water years, river stage trends are similar year to year (Stahl et al., 2016).

2.5. Additional Data Sets

In addition to the survey completed, we also compiled a comprehensive data set for representative end-member stable isotopic values with precipitation isotopic values collected and determined in 2003 and 2004 at the Institute of Nuclear Science and Technology in Hanoi, precipitation and river values given by the Global Networks of Isotopes in Precipitation, and Global Networks of Isotopes in Rivers retrieved through the Water Isotope System for Data Analysis, Visualization and Electronic Retrieval database, and previously published studies in the Red River Delta near Hanoi (Berg et al., 2008; Dang et al., 2010; Kuroda, Hayashi, Do, et al., 2017; Postma et al., 2017; Stahl et al., 2016). Precipitation data for August 2016 to October 2017 were obtained from Precipitation Estimation from Remotely Sensed Information using Artificial Neural Networks system from the University of California Irvine Center for Hydrometeorology and Remote Sensing, which quantifies rainfall rate via remote sensing (Maggioni et al., 2016).

2.6. End-Member Mixing Model of Recharge Sources

A three-end-member model was constructed with values of $\delta^{18}O$ and $\delta^{2}H$ to account for the main sources of recharge to groundwater (gw): fresh precipitation (i.e., short residence time surface water), pond and surface waters (i.e., nonriverine standing water with longer residence time that includes both pond and sewage), and riverine recharge by rearranging equations (1)–(3) to equations (4)–(6) (supporting information, SI). Here, the end-member of surface water includes both ponds and sewage instead of sewage only as an individual source as sewage commonly discharges to surface water bodies such as ponds.

$$f_{\mathrm{gw}} = 1 = f_{\mathrm{river}} + f_{\mathrm{surface\ water}} + f_{\mathrm{precip}} \tag{1}$$

$$\delta^{18}O_{\mathrm{gw}} = f_{\mathrm{river}}\delta^{18}O_{\mathrm{river}} + f_{\mathrm{surface\ water}}\delta^{18}O_{\mathrm{surface\ water}} + f_{\mathrm{precip}}\delta^{18}O_{\mathrm{precip}} \tag{2}$$

$$\delta^{2}H_{\mathrm{gw}} = f_{\mathrm{river}}\delta^{2}H_{\mathrm{river}} + f_{\mathrm{surface\ water}}\delta^{2}H_{\mathrm{surface\ water}} + f_{\mathrm{precip}}\delta^{2}H_{\mathrm{precip}} \tag{3}$$

$$f_{\mathrm{precip}} = \frac{\delta^{2}H_{\mathrm{gw}} - \delta^{2}H_{\mathrm{river}} - f_{\mathrm{surface\ water}}\left(\delta^{2}H_{\mathrm{surface\ water}} - \delta^{2}H_{\mathrm{river}}\right)}{\delta^{2}H_{\mathrm{precip}} - \delta^{2}H_{\mathrm{river}}} \tag{4}$$

$$f_{\mathrm{river}} = \frac{\delta^{18}O_{\mathrm{gw}} - \delta^{18}O_{\mathrm{precip}} - f_{\mathrm{surface\ water}}\left(\delta^{18}O_{\mathrm{surface\ water}} - \delta^{18}O_{\mathrm{precip}}\right)}{\delta^{18}O_{\mathrm{river}} - \delta^{18}O_{\mathrm{precip}}} \tag{5}$$

$$f_{\mathrm{surface\ water}} = 1 - f_{\mathrm{precip}} - f_{\mathrm{river}} \tag{6}$$

It is important to note that no singular end-member value defines a given recharge source. Instead, in this case, fresh rainfall recharge, riverine recharge, and surface water recharge all have isotopic compositions that vary temporally, and to some extent spatially, over the study area. Thus, each recharge source has a number of potential end-member compositions and the best model should not depend on a single end-member but a distribution of potential end-members that may be hydraulically constrained (Movie S1). Thus, we use a two-step Monte Carlo simulation that (1) identifies a number of viable end-members and their combinations from measured water isotopic compositions in specific sources and (2) varies these viable end-members to generate an ensemble of potential end-member combinations from which the fractions of each groundwater composition are estimated (Table S1). This is then repeated for each combination of the viable end-member compositions defined in the first step as demonstrated by Figure S1.

In Step 1, we identify a number of potential combinations of end-members that are both consistent with measured hydrological heads and that describe most of the data. From multiple realizations of potential isotopic end-members values, potential isotopic end-member distributions of $\delta^{18}O$ and $\delta^{2}H$ were chosen based on the seasonality of the recharge source considered. Fortunately, many end-members can be eliminated from consideration based on seasonal trends in heads. For example, riverine recharge varies from −10‰ to 0‰ $\delta^{18}O$ from rainy to dry season due to evaporation in the dry season and dilution from fresh precipitation. Of these, the heaviest of the isotopic compositions are present when the river stage is still generally low at the beginning of monsoon season before it increases markedly later in the monsoon season (Figure 3). Thus, the relatively low river stage is unfavorable for recharge except in a few areas where local pumping occurs. Given this limit on riverine recharge end-member composition, it is also possible to better describe surface water

composition. Only combinations of (a) very light surface water and very heavy river water or (b) very heavy surface water and very light river water can describe the bulk of groundwater compositions. Scenario (a) is hydraulically unlikely as recharge is more likely to occur during the monsoon season when river water is isotopically lighter. Thus, the riverine recharge end-member must be light isotopically light, and, in turn, surface water (ponds) recharge is isotopically heavy. This is consistent with when most recharge is expected from ponds (viz., toward the end of the dry season when ponds have a relatively heavy isotopic composition due to evaporation).

The end-member range for river water was thus chosen as the minimum possible riverine isotopic composition, found during the later monsoon season in September, because rivers only recharge aquifers when the river stage is high enough to recharge the lower groundwater table (Stahl et al., 2016). The river stage is also influenced by upstream dams as during the dry season some of the water may be stored or diverted for irrigation or open during floods, which may also affect whether the river stage is high enough to recharge the aquifer (Dang et al., 2010; Le et al., 2007). While groundwater in some regions of Hanoi may experience increased riverine recharge recently due to the Hanoi drawdown cone as discerned by water level measurements, for most aquifers, the recharge from river to aquifers is more likely to be seasonal, especially preperturbation (Berg et al., 2008). The increased river stage coincides with the increased dilution of the riverine isotopic composition from the isotopically lighter precipitation upstream and produces the riverine isotopic composition minimum as depicted by the example hydrograph (Figures 3 and S2). This river end-member value was obtained from the intersection between the global meteoric water line, assumed to be generally representative of inland precipitation, and the river "water line" as the minimum riverine isotopic composition possible should be derived from where the two lines intersect (Clark & Fritz, 1997). Although we also take the resulting fraction riverine recharge to mainly represent fraction Red River recharge, it is generalizable to the regional Hanoi area as fraction riverine recharge from rivers with similar headwaters including smaller rivers and tributaries have closely similar isotopic composition (Figure S13). Finally, fresh precipitation is similar to surface water recharge with the predominant difference being the residence time, or time spent on the surface before recharge to groundwater, of the water. The fresh precipitation end-member isotopic composition was selected as monthly weighted average precipitation to account for monthly variations in amount of precipitation (SI Text S1).

From a list of 30 potentially reasonable models (Table S1), 18 end-member combinations are rejected because they resulted in models describing less than 60% of the groundwaters sampled. A particular model was considered successful if it described at least 60% of the groundwaters sampled; the majority of successful models described between 70% and 80% of groundwater samples and no models described greater than 90% of groundwater samples. The lack of a model describing all of the data reflects the fact that models are restricted to observed values rather than extremes and that there are likely to be more than three singular end-members across such a wide study area. We then retain this entire set of 12 end-member combinations describing more than 60% of groundwater data to model the fractions of each recharge source (Figure S3). All incorporated end-member models investigated in this step thus have this combination of light riverine recharge and heavy surface water, though we investigate a range of specific values of each in modeling (Movie S1). Only a small portion of groundwater samples can be described if the riverine recharge is heavier than $-8‰$ $\delta^{18}O$ so models that are carried forward all have light riverine recharge.

In Step 2, we generate an ensemble of modeled source attribution for each of the 12 retained end-member combinations retained from Step 1. For each of the potential end-member compositions, we generate a set of randomly determined and uniformly distributed (independent and identically distributed) isotopic compositions around each of the above-defined end-members. In this case, we use an approximate distribution of $\pm 1‰$ $\delta^{18}O$ and $\pm 3‰$ $\delta^{2}H$ around the end-member composition identified in Step 1 to reflect possible variance in the true value from measured values without allowing the values of end-member isotopic composition stray such that it no longer is effective in describing much of the data. Using 10 potential values for each end-member yields 1,000 combinations of end-members for each of the Step 1 models, for a total of 12 models * 1,000, or 12,000 model realizations in all. The final fraction of each recharge source (riverine, precipitation, and surficial water) for a particular groundwater sample is determined by generating a histogram of the fraction of recharge determined from each realization within the ensemble. The mode of the histogram (determined to be a better descriptor than the mean or median as it is the most likely/probable value) is taken as the representative fraction recharge for that particular groundwater sample by computing the maximum of

the density of fraction recharge histogram. Recharge source values were then also normalized to unity. This histogram also provides an estimate of the potential uncertainty of each source contribution from the standard deviation (Figure S4).

We also evaluated the effect of performing the Monte Carlo method to evaluate larger uncertainty around ensemble models considered from Step 1. In general, doubling the uncertainty in Step 2 did not appreciably change the calculated modal fraction of a recharge source, did not affect the rank order of samples with a given recharge source and only slightly increased the uncertainty in the result (SI Text S1 and Figures S6 and S7). A comparison is also made to a likely end-member model scenario where one (singular) set of values per recharge source is used to determine how well they agree (Figures S8 and S9).

To distinguish between pond and sewage in the combined end-member of surface water, we used an underlying two-end-member model based on only Cl concentrations (SI Text S2 and Figure S11). Although individual ponds themselves may vary, Cl concentrations in ponds are an order of magnitude lower than that of sewage (McArthur et al., 2012). The temporal variability within a year for ponds is also much smaller and remains at least an order of magnitude lower than sewage Cl concentrations. The final fraction of sewage (equation (7)) is given by the normalized fraction of surface water from the three-end-member model (equation (6)) multiplied by fraction sewage found via the two-end-member model via Cl and similarly for the final fraction of pond (equation (8)).

$$f_{\text{sewage}} = \frac{\text{Cl}_{\text{gw}} - \text{Cl}_{\text{pond}}}{\text{Cl}_{\text{sewage}} - \text{Cl}_{\text{pond}}} * f_{\text{surface water}} \tag{7}$$

$$f_{\text{pond}} = \left(1 - f_{\text{sewage}}\right) * f_{\text{surface water}} \tag{8}$$

Using Br concentrations, or Cl/Br ratios, produced similar results but was more prone to error since many of the water samples had Br concentrations at or near the limits of detection.

3. Results

3.1. Spatial Heterogeneity of Arsenic and Geochemical Parameters

Arsenic is spatially heterogeneous but high overall in the study area (Figure 1a). Only 29.2% of the household well waters randomly sampled in the regional sampling survey are below the World Health Organization guidelines of 10 μg/L and 39.3% are above the Vietnamese standard of 50 μg/L. High arsenic is found on both the western (Hanoi) and eastern (less populated) side of the river.

The δ^2H, δ^{18}O, chloride, and bromide (Cl/Br) ratios of groundwater are conservative parameters that are useful to establish water provenance. Their concentrations are also spatially heterogeneous but broadly vary with distance from the Red River. Some of the lightest (most negative) groundwater δ^{18}O values are found in the river and in groundwater samples closer to the river (up to −10‰), while heavier groundwater δ^{18}O values are generally found in groundwater further away from the river (Figure 1b). This is consistent with orographic differences in water sources, with heavy local waters reflecting local rainfall and lighter isotopes in river water reflecting source water from higher elevations. Similarly, the concentrations of halides in groundwater also vary strongly with orographic source with high levels near the sea to low levels inland, as halide aerosols from seawater rain out early from clouds (Davis et al., 1998; Winkel et al., 2011). This effect is most easily observed with Br concentrations because human activities can preferentially enrich water, particularly sewage, with chloride. As a result, both Br and Cl/Br ratios follow the same general spatial trend as is observed for the water isotopes (Figures 1c and S10). The lowest Br concentrations are found in river water and groundwater samples adjacent to the river, and the highest Br concentrations is found several kilometers from the river on the western bank of the river. This trend in Br concentrations has also been observed regionally in the Red River Basin (Winkel et al., 2011). Br concentrations also can be influenced by the decomposition of Br-containing natural organic matter (Desbarats et al., 2014). This effect is likely significant primarily in environments dominated by riverine recharge, which contains low (near detection limit) Br due to the rainout before the river's inland source. However, Br likely still behaves primarily as a conservative tracer because Cl concentrations vary due to human inputs more than do Br levels (Figure 1d).

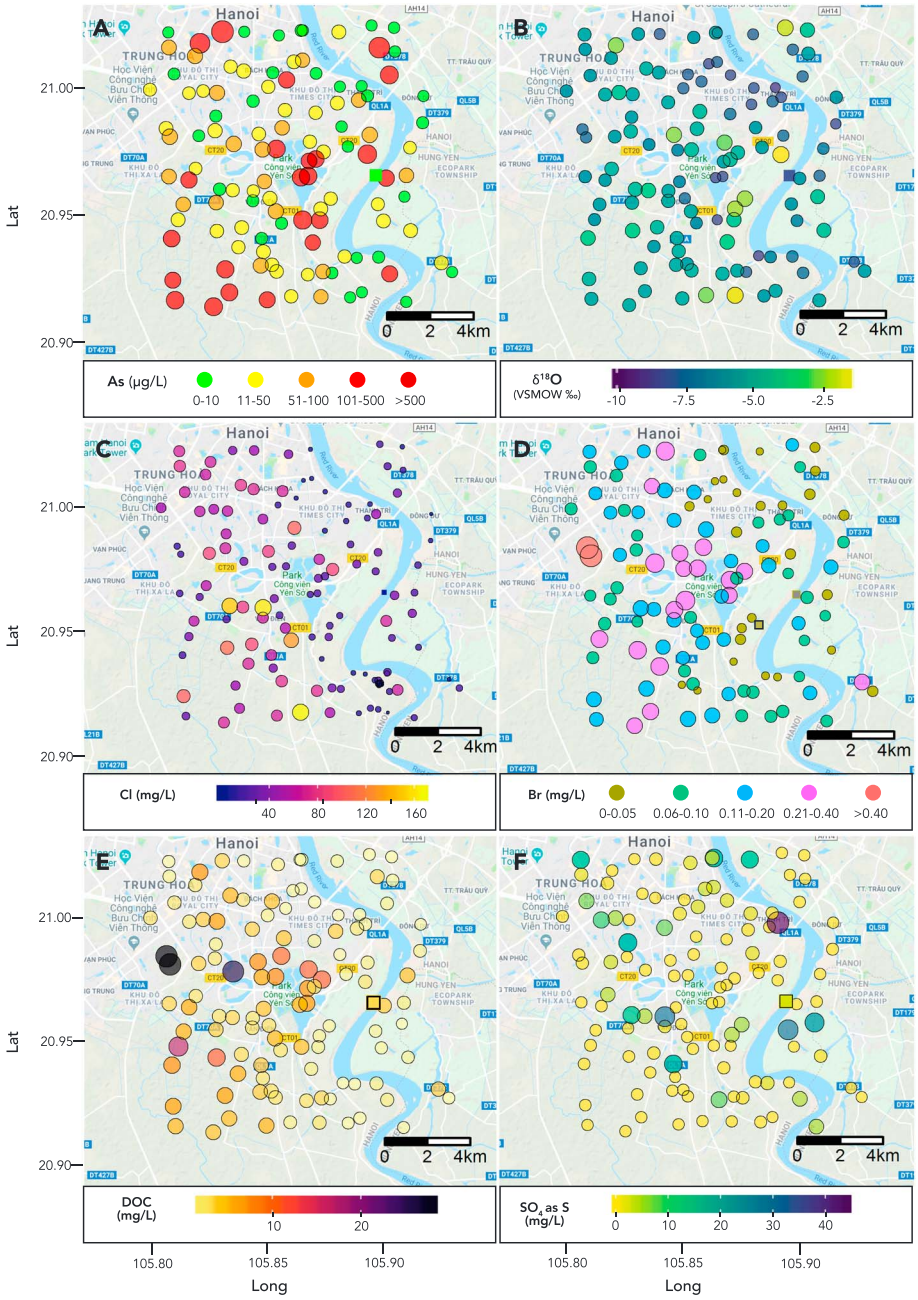

Figure 1. Spatial distribution of (a) groundwater arsenic, (b) $\delta^{18}O$, (c) Cl, (d) Br, (e) DOC, and (f) sulfate-S within the regional sampling area near Hanoi. Groundwater from the initial domestic well sampling survey (December 2013 to May 2014) are shown here and are indicated by circles scaled by value (additional data sets, including high-density sampling points in Van Phuc, not displayed). Average river values are indicated by a square, also scaled with value. The base map is from Google Maps imagery plotted with the R package ggmap (Kahle & Wickham, 2013). DOC = dissolved organic carbon; VSMOW = Vienna Standard Mean Ocean Water.

Spatial heterogeneity in groundwater tracer concentrations reflects considerable differences in the in recharge source. Here, the heterogeneities between each of the tracers show large differences in the sources of recharge locally to the aquifer system, and that underlying geochemical spatial heterogeneity reinforces the potential for and importance of modeling the fraction of recharge from various sources infiltrating the aquifers. Finally, while DOC and sulfate concentrations appear random, DOC concentrations appear to contain some similarities with Br in addition to clusters of high values near ponds for DOC potentially related to Br release from organic matter (Desbarats et al., 2014; Figure 1e). Other anthropogenic sources can include

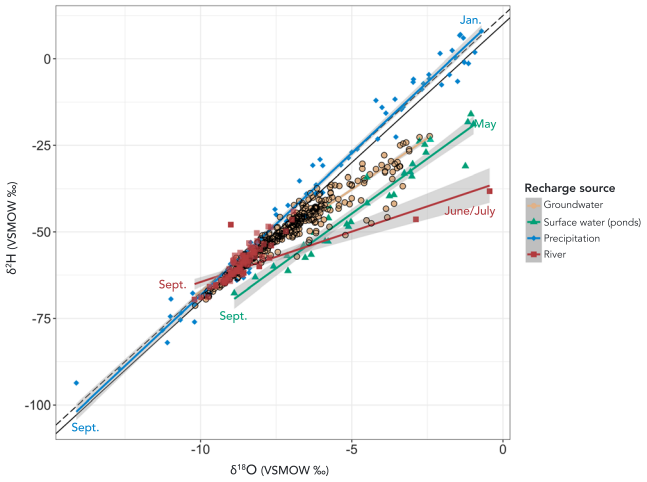

Figure 2. Isotopic composition (δ^2H and $\delta^{18}O$) of ground, surface, and rain water in the Hanoi area relative to the global (solid black line) and local meteoric water line (dotted blacked line). The fitted lines to pond, river, and groundwater data are from linear regression. Standard errors are in gray; for groundwater, the standard error is smaller than the size of the point. Months of maximum and minimum isotopic composition for each water body are noted. VSMOW = Vienna Standard Mean Ocean Water.

latrines, with signature similar to raw sewage. Multiple sulfate sources, including oceanic aerosols and local sulfur dioxide emissions, may contribute to obscure any readily apparent trend for sulfate (Figure 1f). Although Hanoi pumping primarily affects the west bank sites, it is difficult to see whether this perturbation has affected the tracer concentrations, and thus, the potential asymmetry in recharge source between the east and west bank that could result.

3.2. Stable Water Isotopes

3.2.1. Recharge Sources

The water isotopic composition of precipitation was highly variable but fell very close to the global meteoric water line and local meteoric water line (LMWL; Figure 2). Generally, the seasonality in rainfall is reflected in the lighter isotopic signature from the warm, humid, and wet season in September as warmer air masses can hold more water, while the heaviest isotopic signature occurs in the middle of the cool and dry season in January due to increased fractionation (Berg et al., 2008; Dang et al., 2010; Gat, 1996). River values of $\delta^{18}O$ and δ^2H vary seasonally. The mainly light isotopic composition of the river water reflects its source region upstream, where precipitation is composed of lighter isotopes due to rain out that contribute to the headwaters of the Red River. Local evaporative effects near Hanoi also slightly modify the river isotopic signature. Here, the lightest riverine isotopic composition align very closely with the LMWL in Hanoi, despite being derived from the upstream catchment more inland and at higher altitudes in the mountainous Yunnan province in China (Dang et al., 2010). Although the rainy season begins in May, the heavy June and July $\delta^{18}O$ and δ^2H values fall below the LMWL (Figure 2). This is characteristic of evaporated water bodies either stored in the vadose zone or shallow groundwater due to a lag time for river waters from the upstream source to reach Hanoi or dams storing and then releasing shallow water pre-monsoon and during the early monsoon season (Genereux & Hooper, 1998; Kirchner, 2003). In September, at the conclusion of the wet season, riverine $\delta^{18}O$ and δ^2H are at their isotopically lightest values. Pond isotopic compositions are consistently below the LMWL and aligned to evaporation with heavier $\delta^{18}O$ and δ^2H, which matches well with the evaporation line for the average annual humidity of 78% in Hanoi (Berg et al., 2008; Clark & Fritz, 1997). Similarly, pond seasonality shows the isotopically lightest values of $\delta^{18}O$ and δ^2H at the conclusion of a rainy, wet season in September due to dilution by isotopically lighter precipitation influx and becomes isotopically heavier due to evaporation over dry season (Berg et al., 2001; Dansgaard, 1964 ; Gat, 1971 ; Gonfiantini, 1986).

3.2.2. Groundwater

Groundwater $\delta^{18}O$ and δ^2H composition fall close to, or beneath, the LMWL, intersecting the LMWL and riverine "water line" around $\delta^{18}O$ of −9‰ and δ^2H of −60‰ (Figure 2). Groundwater under the meteoric water line in general is characteristic of waters that have experienced evaporation, because oxygen and hydrogen fractionate differently due to kinetic isotopic effects when compared to equilibrium fractionation (Dansgaard, 1964; Gat, 1971; Gonfiantini, 1986). Accordingly, the isotopic composition of groundwater reflects the integration of recharge sources over time (Gat, 1971).

3.3. Constraining Recharge Sources With Hydrology

Both the seasonality of the stable isotopic composition of river and ponds recharge and representative Red River water levels vary in response to the presence of the monsoon season (Figure 3). Because groundwater isotopic composition is relatively constant, all groundwater data have been pooled regardless of sampling date (data not shown). Monthly averages of groundwater isotopic composition of $\delta^{18}O$ were consistently −6‰ to −8‰, with minor variations in means reflecting sampling from different well populations. The groundwater isotopic composition of each well, however, should reflect the source(s) and seasonal timing of the recharge (Figure 3).

Recharge is most significant when hydraulic head gradients are greatest between groundwater and the water source. Rivers have widely variable water levels, and as such are only episodic recharge sources and often

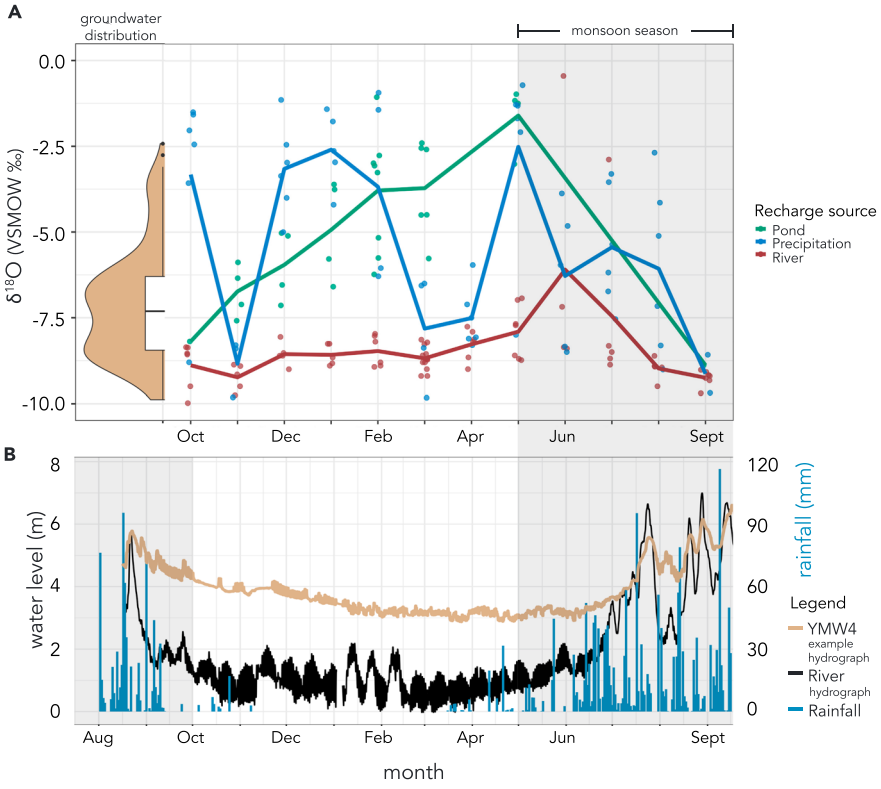

Figure 3. Monthly variation in isotopic composition of recharge sources compared against monthly changes in the Red River water level and hydrograph of a "representative" groundwater well in absolute elevations (m), and rainfall (mm, right axis) during the 2016–2017 water year (supporting information Text S1). The monsoon (or "wet season") is approximately indicated by the gray shaded area. Variations in recharge isotopic composition are compared to the non-variant groundwater isotopic composition distribution, whose composition is represented by the recharge sources. Bolded recharge source lines indicate a moving average. For the isotopic composition, all error bars in figures are smaller than size of symbol. See Figure S2 for location of YMW4. VSMOW = Vienna Standard Mean Ocean Water.

can be sites of discharge. Recharge from rivers occurs disproportionately when river levels are high during the monsoon (Stahl et al., 2016) or in response to groundwater pumping induced shifts in flow (van Geen et al., 2013; SI Text S1).

In contrast, local surface water bodies such as ponds and locally sourced streams have surface elevations that are relatively stable and thus are expected to recharge more in the dry season when groundwater levels are low. This isotopic composition of that surface water or precipitation should also be typical of dry season sources but affected by evaporation or by clogging that slow or stop recharge to groundwater. Each surface water body or pond could conceivably have its own isotopic composition; however, most surface water bodies such as ponds are likely to have similar isotopic composition because they are filled with similar local precipitation and affected similarly by evaporation. All are initially filled with local sources containing a similar regional isotopic composition. Evaporation from those bodies is primarily a function of humidity and temperature, which are also regionally similar. As such, surface water bodies should have $\delta^{18}O$ and $\delta^{2}H$ that lie on a line with a slope determined by that evaporation rate and their position on the line determined by fraction of water that evaporates from the water body (largely determined the surface water body depth; Clark & Fritz, 1997; Gat, 1971). In general, from the seven ponds measured including four ponds measured seven to eight times over a year, surface waters fall on a line and are consistently below at the LMWL.

Based on their physical hydrology, we can identify which recharge sources are important over the wet (approximately May to October) and dry season (approximately November to April; Dang et al., 2010). Riverine recharge likely dominates during the wet season when light upstream and local precipitation dominates its composition. Peaks in the Red River water levels coincide with the timing of minimum isotopic

composition of the river and when anion concentrations are also diluted by this fresh precipitation. During this period, $\delta^{18}O$ is approximately −7.5‰. The evaporative effects on pond isotopic composition are evident over the course of the dry season. During the rainy season, evaporated, heavy pond waters are diluted by fresh, light precipitation. However, we expect recharge to be most significant in dry seasons when the head difference between surface water and groundwater is greatest. From differentiation of these sources, multiple distributions and combinations of potential end-members were determined (SI Text S1).

4. Discussion

4.1. End-Member Modeling of Recharge Sources

4.1.1. Quantification of Recharge Sources

The fraction of precipitation, surface water (pond/sewage), and riverine recharge is determined from the modes of the histograms produced using ensemble modeling for each sample. In general, the majority of recharge in aquifers found in the regional study area can be explained by the ensemble model, meaning the Monte Carlo simulation of multiple distributions of end-members was able to capture a fraction recharge for 174 out of the 183 groundwater samples (95.1%). The standard deviation of each recharge source was taken as the mean standard deviation over all groundwater samples' histograms for a particular recharge source: ±0.109 for fraction riverine recharge, ±0.102 for fraction precipitation recharge, and ±0.051 for fraction surface water recharge (SI Text S1). Since the modes are taken as the most probable fraction recharge, it should be noted that there is no constraint on the sum of calculated fractions, so it need not add to unity. However, the sum is a useful measure of the fit quality. The majority of fraction recharge from river water, precipitation, and surficial water still sum up close to 1 (fraction summing between 0.90 and 1.10) for all groundwater samples modeled (Figure S5). For geochemistry relationships, only groundwater samples with modeled recharge source fraction that sum up to 1.0 ± 0.1 are included (which gives 162/183 samples or 88.5%). We then used the normalized values to relatively compare the different recharge fractions.

4.1.2. Spatial Distribution of Recharge Sources

The spatial variability in recharge sources as determined by fraction of surface water (nonriverine, i.e., pond and sewage), fresh precipitation, and Red River recharge from the model also provides a qualitative verification of end-member modeling where unique RGB values are assigned per percent recharge source (red = Red River, green = surface water, and blue = fresh precipitation; Figure 4). We can discern that most recharge dominated by riverine recharge lie close to the Red River by the inverse relationship between fraction river and distance from river, while aquifers dominated by surficial water bodies are more heterogeneous and scattered, most likely on the availability of surficial waters to recharge (Figure S14). In particular, fraction of pond recharge does not correlate with river distance as pond recharge instead depends upon the heterogeneous distribution of ponds over the survey area (Figure S14). Similarly, sewage sources are point sources and do not display a notable correlation. The remaining aquifers are recharged by short residence time standing water (fraction fresh precipitation), which increase with distance away from the river (Figure S14). Dominance of a certain recharge source indicates not only the availability of the source but also its ability to permeate the subsurface to reach the aquifer that could give an indication of subsurface structure.

4.2. Relation of Recharge Source Variations to Groundwater Geochemistry

4.2.1. Relation Between Recharge Source and Groundwater Arsenic

Although the increasing concentration categories or classes of arsenic as defined in Figure 5 do not appear to have significantly different recharge compositions, consideration of the geochemical parameters with increasing arsenic concentrations alongside fraction recharge is critical to understanding potential arsenic release.

From the model, we find a combination of riverine recharge, surface water, and precipitation recharging the aquifers (Figure 5). Their distinct compositions impact groundwater aquifer composition and redox state. More importantly, these variable sources carry different concentrations of important geochemical variables, such as sulfate or DOC, capable of influencing dissolved arsenic concentrations. Average arsenic concentrations in river water (4.27 μg/L) are much lower than in average arsenic concentrations in groundwater (92.4 μg/L), which indicates arsenic mobilization occurs along the flow path into or within the aquifer and is not being transported from the river water itself.

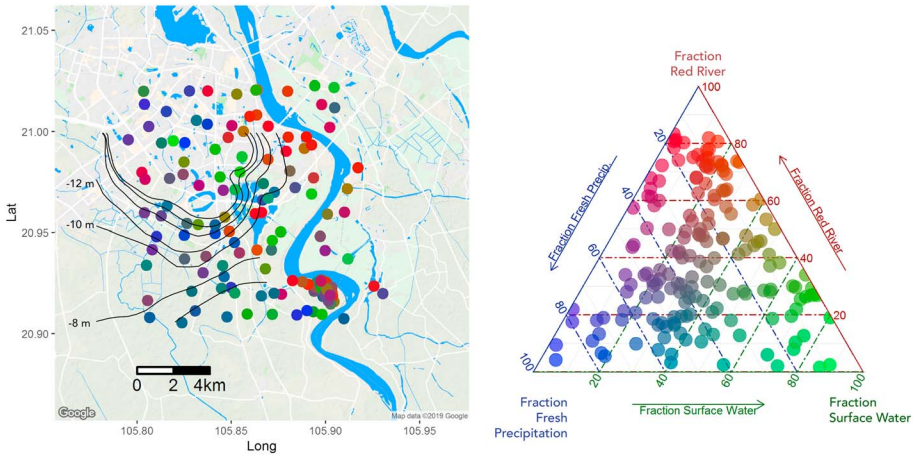

Figure 4. Spatial variability of recharge sources where red is Red River recharge, blue is fresh precipitation, and green is surface water. Hanoi cone of depression is indicated by 2-m groundwater table contours in black (adapted from Berg et al., 2008, and van Geen et al., 2013). Legend for spatial map is given by RGB colors on ternary diagram. Groundwater samples that are not described by the ensemble members are omitted. The base map is from Google Maps imagery. Ternary diagram made with R package ggtern (Hamilton & Ferry, 2018).

4.2.2. Relationship Between Recharge Source, DOC and Groundwater Arsenic

Different sources of recharge have the potential to contain both different amounts of arsenic but also different concentrations and qualities (reactivities) of DOC and thus lead to varying levels of arsenic in groundwater. Here, we focus our attention on the relationship between total DOC and fraction recharge. DOC levels are highly variable but those levels decrease considerably as the fraction of riverine recharge increases (Figures 6a and 7); we thus infer that riverine recharge does not contain a high concentration of DOC once it reaches the aquifer and that the variability in the total DOC reflects more variable inputs in nonriverine recharge sources. From this, we introduce two distinct populations of wells: (Case A) those with low (<50%) riverine recharge and (Case B) those with majority (>50%) riverine recharge. The DOC concentration is significantly different ($p < 0.05$, based on Kruskal-Wallis test) for low riverine recharge samples (Case A) versus high riverine recharge samples (Case B; Figure S15). In this study, Case A consists of groundwater derived from other recharge sources that often contains much higher DOC levels than in Case B with typically low DOC in waters (<2 mg/L; Figure 7). Across both Cases A and B, groundwater with low dissolved Fe typically contain have <10 μg/L arsenic and low DOC (Figure S19).

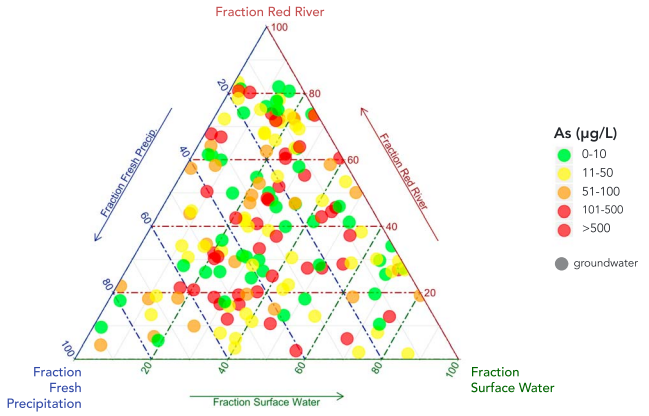

Figure 5. Ternary diagram of three end-member recharge sources of fresh precipitation, surface water, and river in groundwater samples categorized by arsenic concentrations.

4.2.2.1. Case A, Wells With Low Riverine Recharge

Differences in DOC and recharge sources also affect arsenic levels. For Case A, high arsenic (>100 μg/L) containing groundwater is associated with higher DOC (up to 10 mg/L DOC) most dramatic where fraction riverine recharge <0.25 and consistent with OC driving reduction and subsequent arsenic release (Figures 6 and S16). Case A groundwaters are also found with higher dissolved Fe (Figure S19). Dissolved ammonium is a product of OC decomposition in general, and it is often found to increase with groundwater arsenic concentrations because they are both coupled to Fe reduction (e.g., Harvey et al., 2002; Polizzotto et al., 2008; Postma et al., 2007). Although we do not distinguish here what part of the process it comes from, high DOC from solid organic matter degradation can indicate that extensive arsenic reduction has occurred within the sediments, with the potential for more reduction to occur from DOC decomposition (Berg et al., 2008).

In Case A groundwaters, dissolved ammonium concentrations indeed also appear to generally increase with increasing arsenic

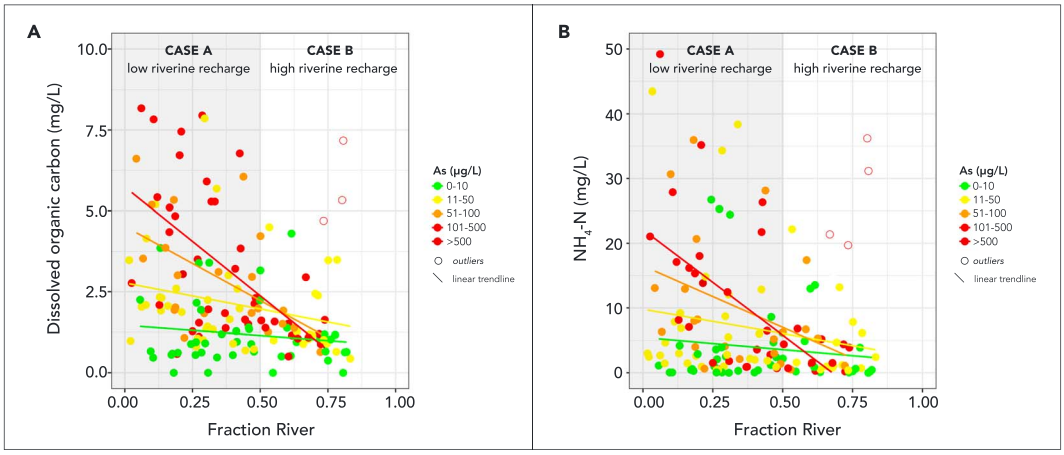

Figure 6. (a) Dissolved organic carbon versus fraction recharge contribution of riverine recharge. Case A, low (<50%) riverine recharge, is shaded in gray with Case B, high (>50%) riverine recharge, in white. Within each category of arsenic concentration (0–10, 11–50, 51–100, 101–500, including >500 µg/L As), riverine recharge shows an inverse linear relationship with dissolved organic carbon in the system when considering realistic dissolved organic carbon (DOC) values under 10 mg/L as in Case A. In Case B, DOC levels remain close to each other nearly no matter the category of arsenic concentration. Outliers above 1.5 times the interquartile range and determined by an outlier test are either delineated by outlined circles or are not plotted, since they are greater than 10 mg/L DOC. (b) Ammonium versus fraction riverine recharge, colored per arsenic category. Only groundwater samples with a valid fraction recharge are included. Outliers above 1.5 times the interquartile range are delineated by outlined circles or are not plotted, since they are greater than 10 mg/L DOC.

concentrations, which may be most dramatic and evident for fraction riverine recharge <0.25 (Figures 6b and S17). The DOC driving iron reduction could have been derived from the advected recharge sources or from in situ carbon. However, there are only weak relationships between DOC concentrations and high nonriverine recharge sources (Figure S18), suggesting an important in situ sedimentary source of OC to the aquifer. For example, the high arsenic, high-DOC region in the southwest of study area away from the riverbank contains extensive peat layers that may be the source of OC and NH_4^+ from decomposition (Berg et al., 2008). Furthermore, Berg et al. (2008) maps NH_4 concentrations that strongly corroborate high NH_4 from high OC decomposition (Figure 6).

4.2.2.2. Case B, Wells With High Riverine Recharge

To then understand the effects of DOC from riverine recharge on arsenic levels in Case B, we need to consider the riverbank geochemistry. Stahl et al. (2016) found that in areas of recent deposition, riverbank pore waters can be highly elevated in arsenic due to extensive iron reduction and rapid arsenic release within depositional riverbanks that ultimately are the source of riverine recharge, partially because they contained both abundant OC and reactive iron oxides. Also, older sediments may lack the reactive Fe oxides and/or sediment arsenic for Fe reduction and arsenic release (Postma et al., 2017; Stahl et al., 2016). Thus, the occurrence of high arsenic in recharging river water is strongly dependent on the geologic conditions of the riverbank sediments.

For Case B, groundwater rich in high riverine recharge contains much lower DOC and ammonium concentrations at equivalent arsenic levels. We infer from these observations that only small quantities of DOC are needed to release arsenic from riverbank sediments into recharge. In riverbanks, there is abundant sedimentary organic matter that contributes to reduction, so this would be expected. This redox process would also produce some dissolved iron and ammonium. However, the modest levels of both indicate that Fe (II) and ammonium are either retained or consumed in the solid phase within these shallow systems.

Within Case B, there are some outliers (Figure 6, outlined circles) that have much greater DOC levels than the mean. The additional DOC in these outliers is most likely not from river water but instead from in situ (sedimentary) or minor recharge sources such as sewage or pond water that contain high DOC. In most areas, local geological data would be helpful to establish which of these contribute DOC. For example, Hanoi sewage is discharged near Yen My and contains elevated DOC. Peats and other sedimentary DOC sources also can influence DOC, ammonium, and arsenic levels (Figures 6a and 6b; Berg et al., 2008; Norrman et al., 2015).

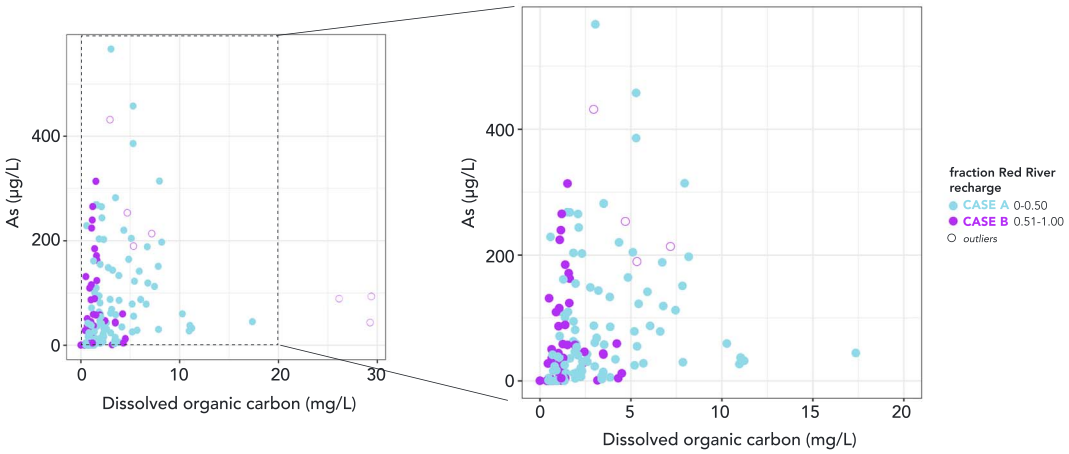

Figure 7. Dissolved arsenic concentrations versus dissolved organic carbon concentrations and grouped by fraction of riverine recharge. Groundwater containing >50% riverine recharge usually contains less than 2–3 ppm dissolved organic carbon (Case B, purple), while groundwaters from other sources (<50% riverine recharge) contain higher dissolved organic carbon levels (Case A, blue). Only groundwater samples with a valid fraction recharge are included. Outliers above 1.5 times the interquartile range are delineated by outlined circles.

Sedimentary geology and geomorphology affect the distribution of arsenic available for release. All groundwaters contain some Fe (II) and thus indicate extensive reduction. However, not all groundwaters contain arsenic, in part because arsenic is depleted from some sediments due to rapidly flushing. Thus, riverine recharge will contain elevated arsenic when derived from recently deposited sediments that still contain abundant arsenic (Postma et al., 2017; Stahl et al., 2016). Although it is difficult to establish the recharge location for most samples, this relationship is clear in sampling from Van Phuc, which has been extensively studied (e.g., Stahl et al., 2016; van Geen et al., 2013). In Van Phuc, high arsenic groundwaters containing riverine recharge are located principally near or in depositional environments, while low arsenic groundwaters containing riverine recharge are located within erosional zones. For cases investigated in Van Phuc, sediment history and geomorphology imprint as a noticeable control on top of riverine recharge distribution, further influencing arsenic release. This emphasizes the fundamental utility of modeling recharge source to independently tease apart these various groundwater populations influenced by geological factors such as peat burial and riverbank geomorphology.

4.2.2.3. Pond and Sewage Recharge

Ponds and sewage are often assumed to be rich in DOC and thus a significant potential contributor to Fe reduction and arsenic mobilization. Here, we find considerable DOC in some water samples derived from these sources, but there are no significant correlations between the fractions of pond water or sewage and the DOC or arsenic levels in the studied groundwaters (Figure S18). These data suggest that redox changes associated with these carbon sources do not contribute significantly to arsenic release at this site (Figure S18). In fact, for either groundwater with discernable fraction pond recharge or fraction sewage recharge, the highest concentrations (>10 mg/L) of DOC are more clearly associated with slightly lower to midrange dissolved arsenic concentrations (~11 to 50 µg/L; Figure S18). One explanation for this observation is that one source of DOC, human or animal sewage, contains high nitrate and sulfate, both of which can affect Fe (III) reduction and/or arsenic sequestration (McArthur et al., 2012; Norrman et al., 2015). The studied groundwater samples with greater than 5% fraction of sewage recharge have an average of 8.36 mg/L SO_4 as S, while groundwater with less than 5% fraction sewage recharge only contain 1.75 mg/L SO_4 as S. These groundwaters with fraction sewage greater than 5% and high sulfate waters contain average arsenic of 19.45 µg/L.

4.2.3. Effect of Sulfate on Groundwater Arsenic

Dissolved arsenic concentrations are commonly associated with sulfate concentrations less than a few mg/L (McArthur et al., 2012; Saalfield & Bostick, 2009; Sun, Quicksall, et al., 2016). Since different recharge sources should have distinct sulfate concentrations, the introduction of high sulfate groundwater, for example, from sewage or local oxidation of organic or mineral S, could potentially influence

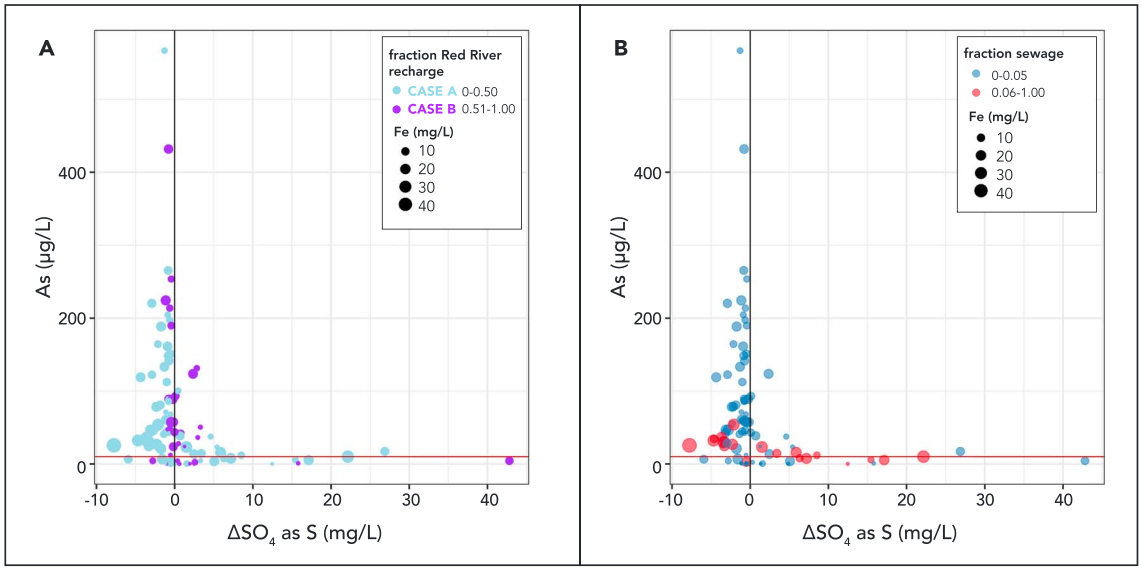

Figure 8. Arsenic versus ΔSO_4^{2-} as categorized by (a) fraction Red River recharge and (b) fraction sewage. Vertical black line indicates sulfate values match predicted sulfate from seawater-freshwater mixing line ($\Delta SO_4^{2-} = 0$). Red line indicates World Health Organization limit for arsenic. All points, colored by two cases of low or high riverine recharge, indicate groundwater samples with the size proportional to concentration of dissolved Fe. Dissolved Fe is indicative of reducing conditions even where ΔSO_4^{2-} is positive (usually thought of as more oxidizing).

groundwater As levels. Sulfate concentrations of 1 mg/L or more generally can sustain appreciable sulfate reduction (Jakobsen & Postma, 1999; Pallud & Van Cappellen, 2006).

In this study, we also find arsenic is associated with low sulfate (Figure S12). To better understand the sources and sinks of S that affect S levels in each groundwater sample, it is often useful to compare measured sulfate levels to sulfate concentrations predicted based on seawater sulfate/chloride ratios (McArthur et al., 2012). This is done using the seawater-freshwater mixing line (equation (9)) as calculated (SI Text S2) similar to McArthur et al. (2012).

$$\Delta SO_4^{2-}\ (\text{excess sulfate}) = \text{measured } SO_4^{2-} - \text{predicted } SO_4^{2-} \qquad \textit{where}$$
$$\text{predicted } SO_4^{2-} = \left(\frac{SO_4^{2-}}{Cl^-}\right)_{\text{sea salt}} {}^*Cl^-_{\text{measured}} = \left(\frac{2,710\frac{\text{mg}}{\text{L}}\,SO_4^{2-}}{19,350\frac{\text{mg}}{\text{L}}\,Cl^-}\right) {}^*Cl^-_{\text{measured}} \tag{9}$$

Here, predicted SO_4^{2-} (as S) is calculated as predicted sulfate as $SO_4^{2-} = Cl/21.4$ when SO_4^{2-} is converted to S (SI equations). Deviation of measured sulfate concentrations from predicted implies that other sources or sinks of sulfate are present. Potential sources can include seawater or sea salt aerosols, sulfur oxide (SO_x) emissions, sewage, and microbial sources among other sources. SO_x emissions here may arise from local traffic pollution or industrial coal burning (Hien et al., 2014), which is oxidized to SO_4^{2-} in the atmosphere. Sinks can include sulfate reduction. Calculation of ΔSO_4^{2-} here accounts for one of the major sources: sea salt aerosols in precipitation.

In general, arsenic concentrations are generally low when sulfate levels are higher than a few milligrams per liter or when ΔSO_4^{2-} is positive (Figure 8). This is usually interpreted as indicative of either persistent oxidizing conditions (where arsenic can remain on stable iron minerals) or sulfate reducing conditions that favor the formation of arsenic sulfide minerals. In this study, positive ΔSO_4^{2-} values were observed in groundwaters that were often reducing (Figure 8), as evidenced by high dissolved Fe levels in these water

samples indicating an iron-reducing environment. However, this reduction does not release arsenic, possibly due to the formation of sulfide minerals in areas where active Fe reduction is occurring (Buschmann & Berg, 2009).

Groundwaters in our study area with high As generally have values of $\Delta SO_4^{2-} < 0$ (i.e., indicative of a loss of sulfate, often reaching concentrations of <1 mg/L; Figure 8). Negative ΔSO_4^{2-} indicates that sinks of sulfate have removed more of the sulfate than would have been added by only one of the sources (seawater). Thus, the high-As waters with negative ΔSO_4^{2-} have been affected by extensive sulfate reduction and/or cycling. This is consistent with extensive sulfate reduction predicating high arsenic concentrations (Bethke et al., 2011; Borch et al., 2010).

It is difficult to relate sulfate or ΔSO_4^{2-} concentrations to recharge source. Although there is no distinct linear relationship with arsenic concentrations, groundwaters with low riverine recharge fractions (Case A) have a wider distribution of ΔSO_4^{2-} than is observed for waters with high riverine recharge fractions (Case B). The consistency of Case B groundwaters implies that inferred sulfate levels are consistent and that sulfate removal by sulfate reduction is widespread in groundwaters dominated by riverine recharge (Figure 8a). The variation in ΔSO_4^{2-} for Case A groundwaters probably reflects considerably more variation in sources and in sinks that affects groundwater sulfate levels. One potential source of sulfate and DOC is sewage, both of which influence arsenic levels (McArthur et al., 2012; Norrman et al., 2015). Both sulfate and ΔSO_4^{2-} in this study are clearly affected by differences in sewage inputs but that those inputs do not necessarily yield high-As groundwater (Figure 8b).

5. Conclusions

From this regional survey in the Red River Delta, we find that groundwater is recharged from surficial water bodies, fresh precipitation, and river water that have seasonality variability in their isotopic signatures. The isotopic composition of these water bodies ($\delta^{18}O$ and $\delta^{2}H$) contributes a distinct isotopic signature to the groundwater aquifers, which maintains a consistent isotopic signature that reflects their recharge sources. From Monte Carlo simulations of end-member modeling with conservative geochemical tracers of $\delta^{18}O$, $\delta^{2}H$, and Cl distribution of values, we find rivers and ponds are also an important contributor with heterogeneous distribution driven by increased groundwater pumping in the expanding Hanoi area. This novel approach allows us to differentiate recharge source in systems where there is considerable variability in end-member compositions in time and space and allows us to connect recharge source information to geochemistry, especially opportune and advantageous for large data sets where networks of hydrographs are much more infeasible.

There appears to be significant recharge from the Red River occurring regionally and frequently associated with high-As groundwater. For each category of increasing arsenic concentration, aquifers dominated by low (<50%) riverine recharge (Case A) have defined correlations between DOC and As concentrations, especially for fraction riverine recharge <0.25. In contrast, aquifers dominated by high riverine (>50%) recharge (Case B) all have lower DOC concentrations that are uncorrelated to As concentrations. This could mean that riverine recharge contains As that is efficiently advected into the aquifers. However, it is important to note that geological heterogeneity along the flow path to the aquifer may exacerbate or reduce groundwater arsenic contamination by adsorbing or desorbing additional As through facilitating additional reduction or creating preferential flow. Sulfate and DOC concentrations also appear to be affected by these processes. Sulfate cycling is evident in most water samples, and much of the sulfate is removed from groundwater, even from waters that contained elevated levels of sewage.

Understanding complex hydrology is difficult in sparse networks but remains essential in understanding groundwater quality since the accurate attribution of recharge sources can help inform water resource management. It is fundamental to consider increased urban water use that creates high gradients for recharge and may disrupt our current understanding of seasonality of recharge as discerned from geochemical parameters. Water pumping affects both local gradients and the sources of recharge and thus could affect water quality. In particular, it is also critical to understand the interactions between surface water and groundwater. From our novel reconstruction of fraction recharge source, we are able to identify the areas where groundwater arsenic concentrations are susceptible to change due to hydrologic disturbances that affect the groundwater quality for millions in this region.

Acknowledgments

This work was supported by National Science Foundation Grant EAR 15-21356, National Institute of Environmental Health Sciences Grant ES010349, Partnerships for Enhanced Engagement in Research (PEER) Project 2-544, and a National Science Foundation Graduate Research Fellowship. This is LDEO Contribution Number 8336. The data can be found on Columbia University Academic Commons (https://doi.org/10.7916/d8-fcq1-hd60). Thank you to Tyler Ellis, Jamie Ross, Marty Fleisher, and Khue Nguyen for productive and supportive laboratory assistance, Viet Nga, Vu Duyen, and Vi Mai Lan for essential field assistance, Dieke Postma for providing valuable isotopic data from his field sites in Vietnam, and the people of Van Phuc for supporting our project. The authors declare no competing financial interests.

References

Berg, M., Tran, H. C., Nguyen, T. C., Pham, H. V., Schertenleib, R., & Giger, W. (2001). Arsenic contamination of groundwater and drinking water in Vietnam: A human health threat. *Environmental Science & Technology*, *35*(13), 2621–2626. https://doi.org/10.1021/es010027y

Berg, M., Trang, P. T. K., Stengel, C., Buschmann, J., Viet, P. H., Van Dan, N., et al. (2008). Hydrological and sedimentary controls leading to arsenic contamination of groundwater in the Hanoi area, Vietnam: The impact of iron-arsenic ratios, peat, river bank deposits, and excessive groundwater abstraction. *Chemical Geology*, *249*(1–2), 91, 112. https://doi.org/10.1016/j.chemgeo.2007.12.007

Bethke, C. M., Sanford, R. A., Kirk, M. F., Jin, Q., & Flynn, T. M. (2011). The thermodynamic ladder in geomicrobiology. *American Journal of Science*, *311*(3), 183–210. https://doi.org/10.2475/03.2011.01

Borch, T., Kretzschmar, R., Skappler, A., Van Cappellen, P., Ginder-Vogel, M., Voegelin, A., & Campbell, K. (2010). Biogeochemical redox processes and their impact on contaminant dynamics. *Environmental Science and Technology*, *44*(1), 15–23. https://doi.org/10.1021/es9026248

Bostick, B. C., Fendorf, S., & Brown, G. E. (2005). In situ analysis of thioarsenite complexes in neutral to alkaline arsenic sulphide solutions. *Mineralogical Magazine*, *69*(5), 781–795. https://doi.org/10.1180/0026461056950288

Burton, E. D., Johnston, S. G., & Kocar, B. D. (2014). Arsenic mobility during flooding of contaminated soil: The effect of microbial sulfate reduction. *Environmental Science and Technology*, *48*(23), 13,660–13,667. https://doi.org/10.1021/es503963k

Buschmann, J., & Berg, M. (2009). Impact of sulfate reduction on the scale of arsenic contamination in groundwater of the Mekong, Bengal and Red River deltas. *Applied Geochemistry*, *24*(7), 1278–1286. https://doi.org/10.1016/j.apgeochem.2009.04.002

Christophersen, N., & Hooper, R. P. (1992). Multivariate analysis of stream water chemical data: The use of principal components analysis for the end-member mixing problem. *Water Resources Research*, *28*(1), 99–107. https://doi.org/10.1029/91WR02518

Clark, I., & Fritz, P. (1997). The environmental isotopes. In *Environmental isotopes in hydrogeology*. Boca Raton, FL: CRC Press. https://doi.org/10.1002/047147844X.gw211

Correa, A., Breuer, L., Crespo, P., Célleri, R., Feyen, J., Birkel, C., et al. (2019). Spatially distributed hydro-chemical data with temporally high-resolution is needed to adequately assess the hydrological functioning of headwater catchments. *Science of the Total Environment*, *651*(Pt 1), 1613–1626. https://doi.org/10.1016/j.scitotenv.2018.09.189

Dang, T. H., Coynel, A., Orange, D., Blanc, G., Etcheber, H., & Le, L. A. (2010). Long-term monitoring (1960-2008) of the river-sediment transport in the Red River Watershed (Vietnam): Temporal variability and dam-reservoir impact. *Science of the Total Environment*, *408*(20), 4654–4664. https://doi.org/10.1016/j.scitotenv.2010.07.007

Dansgaard, W. (1964). Stable isotopes in precipitation. *Tellus*, *16*(4), 436–468. https://doi.org/10.3402/tellusa.v16i4.8993

Davis, S. N., Whittemore, D. O., & Fabryka-Martin, J. (1998). Uses of chloride/bromide ratios in studies of potable water. *Ground Water*, *36*(2), 338–350. https://doi.org/10.1111/j.1745-6584.1998.tb01099.x

Desbarats, A. J., Koenig, C. E. M., Pal, T., Mukherjee, P. K., & Beckie, R. D. (2014). Groundwater flow dynamics and arsenic source characterization in an aquifer system of West Bengal, india. *Water Resources Research*, *50*, 4974–5002. https://doi.org/10.1002/2013WR014034

Dowling, C. B., Poreda, R. J., Basu, A. R., Peters, S. L., & Aggarwal, P. K. (2002). Geochemical study of arsenic release mechanisms in the Bengal Basin groundwater. *Water Resources Research*, *38*(9), 1173. https://doi.org/10.1029/2001WR000968

Fendorf, S., Michael, H. A., & van Geen, A. (2010). Spatial and temporal variations of groundwater arsenic in South and Southeast Asia. *Science*, *328*(5982), 1123–1127. https://doi.org/10.1126/science.1172974

Gat, J. R. (1971). Comments on the stable isotope method in regional groundwater investigations. *Water Resources Research*, *7*(4), 980–993. https://doi.org/10.1029/WR007i004p00980

Gat, J. R. (1996). Oxygen and hydrogen isotopes in the hydrologic cycle. *Earth and Planetary Science*, *24*(1), 225–262. https://doi.org/10.1146/annurev.earth.24.1.225

Genereux, D. P., & Hooper, R. P. (1998). Oxygen and hydrogen isotopes in rainfall-runoff studies. In *Isotope tracers in catchment hydrology* (pp. 319–346). Amsterdam, Netherlands: Elsevier B.V. https://doi.org/10.1016/B978-0-444-81546-0.50017-3

Gonfiantini, R. (1986). Environmental isotopes in lake studies. In *Handbook of Environmental Isotope Geochemistry: The Terrestrial Environment, B* (pp. 113–168). Amsterdam, Netherlands: Elsevier. https://doi.org/10.1016/B978-0-444-42225-5.50008-5

Hamilton, N. E., & Ferry, M. (2018). **ggtern**: Ternary diagrams using **ggplot2**. *Journal of Statistical Software*, *87*(Code Snippet 3). https://doi.org/10.18637/jss.v087.c03

Harvey, C. F., Swartz, C. H., Badruzzaman, A. B. M., Keon-Blute, N., Yu, W., Ali, M. A., et al. (2002). Arsenic mobility and groundwater extraction in Bangladesh. *Science*, *298*(5598), 1602–1606. https://doi.org/10.1126/science.1076978

Hien, P. D., Hangartner, M., Fabian, S., & Tan, P. M. (2014). Concentrations of NO_2, SO_2, and benzene across Hanoi measured by passive diffusion samplers. *Atmospheric Environment*, *88*(2), 66–73. https://doi.org/10.1016/j.atmosenv.2014.01.036

Jakobsen, R., & Postma, D. (1999). Redox zoning, rates of sulfate reduction and interactions with Fe-reduction and methanogenesis in a shallow sandy aquifer, Romo, Denmark. *Geochimica et Cosmochimica Acta*, *63*(1), 137–151. https://doi.org/10.1016/S0016-7037(98)00272-5

Kahle, D., & Wickham, H. (2013). ggmap: Spatial Visualization with. *The R Journal*, *4*(2/3), 193–216. https://doi.org/10.1023/A:1009843930701

Kirchner, J. W. (2003). A double paradox in catchment hydrology and geochemistry. *Hydrological Processes*, *17*(4), 871–874. https://doi.org/10.1002/hyp.5108

Kuroda, K., Hayashi, T., Do, A. T., Canh, V. D., Nga, T. T. V., Funabiki, A., & Takizawa, S. (2017). Groundwater recharge in suburban areas of Hanoi, Vietnam: Effect of decreasing surface-water bodies and land-use change. *Hydrogeology Journal*, *25*(3), 727–742. https://doi.org/10.1007/s10040-016-1528-2

Kuroda, K., Hayashi, T., Funabiki, A., Do, A. T., Canh, V. D., Nga, T. T. V., & Takizawa, S. (2017). Holocene estuarine sediments as a source of arsenic in Pleistocene groundwater in suburbs of Hanoi, Vietnam. *Hydrogeology Journal*, *25*(4), 1137–1152. https://doi.org/10.1007/s10040-016-1527-3

Le, T. P. Q., Garnier, J., Gilles, B., Sylvain, T., & Van Minh, C. (2007). The changing flow regime and sediment load of the Red River, Viet Nam. *Journal of Hydrology*, *334*(1–2), 199–214. https://doi.org/10.1016/j.jhydrol.2006.10.020

Maggioni, V., Meyers, P. C., & Robinson, M. D. (2016). A review of merged high-resolution satellite precipitation product accuracy during the Tropical Rainfall Measuring Mission (TRMM) Era. *Journal of Hydrometeorology*, *17*(4), 1101–1117. https://doi.org/10.1175/JHM-D-15-0190.1

Mailloux, B. J., Trembath-Reichert, E., Cheung, J., Watson, M., Stute, M., Freyer, G. A., et al. (2013). Advection of surface-derived organic carbon fuels microbial reduction in Bangladesh groundwater. *Proceedings of the National Academy of Sciences*, *110*(14), 5331–5335. https://doi.org/10.1073/pnas.1213141110

Majumder, S., Datta, S., Nath, B., Neidhardt, H., Sarkar, S., Roman-Ross, G., et al. (2016). Monsoonal influence on variation of hydrochemistry and isotopic signatures: Implications for associated arsenic release in groundwater. *Journal of Hydrology*, *535*, 407–417. https://doi.org/10.1016/j.jhydrol.2016.01.052

McArthur, J. M., Sikdar, P. K., Hoque, M. A., & Ghosal, U. (2012). Waste-water impacts on groundwater: Cl/Br ratios and implications for arsenic pollution of groundwater in the Bengal Basin and Red River Basin, Vietnam. *Science of the Total Environment*, *437*, 390–402. https://doi.org/10.1016/j.scitotenv.2012.07.068

Norrman, J., Sparrenbom, C. J., Berg, M., Dang, D. N., Jacks, G., Harms-Ringdahl, P., et al. (2015). Tracing sources of ammonium in reducing groundwater in a well field in Hanoi (Vietnam) by means of stable nitrogen isotope ($\delta^{15}N$) values. *Applied Geochemistry*, *61*, 248–258. https://doi.org/10.1016/j.apgeochem.2015.06.009

Oremland, R. S., & Stolz, J. F. (2005). Arsenic, microbes and contaminated aquifers. *Trends in Microbiology*, *13*(2), 45–49. https://doi.org/10.1016/j.tim.2004.12.002

Pallud, C., & Van Cappellen, P. (2006). Kinetics of microbial sulfate reduction in estuarine sediments. *Geochimica et Cosmochimica Acta*, *70*(5), 1148–1162. https://doi.org/10.1016/j.gca.2005.11.002

Polizzotto, M. L., Kocar, B. D., Benner, S. G., Sampson, M., & Fendorf, S. (2008). Near-surface wetland sediments as a source of arsenic release to ground water in Asia. *Nature*, *454*(7203), 505–508. https://doi.org/10.1038/nature07093

Postma, D., Jessen, S., Hue, N. T. M., Duc, M. T., Koch, C. B., Viet, P. H., et al. (2010). Mobilization of arsenic and iron from Red River floodplain sediments, Vietnam. *Geochimica et Cosmochimica Acta*, *74*(12), 3367–3381. https://doi.org/10.1016/j.gca.2010.03.024

Postma, D., Larsen, F., Minh Hue, N. T., Duc, M. T., Viet, P. H., Nhan, P. Q., & Jessen, S. (2007). Arsenic in groundwater of the Red River floodplain, Vietnam: Controlling geochemical processes and reactive transport modeling. *Geochimica et Cosmochimica Acta*, *71*(21), 5054–5071. https://doi.org/10.1016/j.gca.2007.08.020

Postma, D., Larsen, F., Thai, N. T., Trang, P. T. K., Jakobsen, R., Nhan, P. Q., et al. (2012). Groundwater arsenic concentrations in Vietnam controlled by sediment age. *Nature Geoscience*, *5*(9), 656–661. https://doi.org/10.1038/ngeo1540

Postma, D., Mai, N. T. H., Lan, V. M., Trang, P. T. K., Sø, H. U., Nhan, P. Q., et al. (2017). Fate of arsenic during red river water infiltration into aquifers beneath Hanoi, Vietnam. *Environmental Science and Technology*, *51*(2), 838–845. https://doi.org/10.1021/acs.est.6b05065

Richards, L. A., Magnone, D., Boyce, A. J., Casanueva-Marenco, M. J., van Dongen, B. E., Ballentine, C. J., & Polya, D. A. (2018). Delineating sources of groundwater recharge in an arsenic-affected Holocene aquifer in Cambodia using stable isotope-based mixing models. *Journal of Hydrology*, *557*, 321–334. https://doi.org/10.1016/j.jhydrol.2017.12.012

Rowland, H. A. L., Polya, D. A., Lloyd, J. R., & Pancost, R. D. (2006). Characterisation of organic matter in a shallow, reducing, arsenic-rich aquifer, West Bengal. *Organic Geochemistry*, *37*(9), 1101–1114. https://doi.org/10.1016/j.orggeochem.2006.04.011

Saalfield, S., & Bostick, B. (2009). Changes in iron, sulfur, and arsenic speciation associated with bacterial sulfate reduction in ferrihydrate-rich systems. *Environmental Science & Technology*, *43*(23), 8787–8793. https://doi.org/10.1021/es901651k

Stahl, M. O., Harvey, C. F., van Geen, A., Sun, J., Thi Kim Trang, P., Mai Lan, V., et al. (2016). River bank geomorphology controls groundwater arsenic concentrations in aquifers adjacent to the Red River, Hanoi Vietnam. *Water Resources Research*, *52*, 6321–6334. https://doi.org/10.1002/2016WR018891

Suess, E., & Planer-Friedrich, B. (2012). Thioarsenate formation upon dissolution of orpiment and arsenopyrite. *Chemosphere*, *89*(11), 1390–1398. https://doi.org/10.1016/j.chemosphere.2012.05.109

Sun, J., Chillrud, S. N., Mailloux, B. J., & Bostick, B. C. (2016). In situ magnetite formation and long-term arsenic immobilization under advective flow conditions. *Environmental Science & Technology*, acs.est.6b02362. https://doi.org/10.1021/acs.est.6b02362

Sun, J., Chillrud, S. N., Mailloux, B. J., Stute, M., Singh, R., Dong, H., et al. (2016). Enhanced and stabilized arsenic retention in microcosms through the microbial oxidation of ferrous iron by nitrate. *Chemosphere*, *144*, 1106–1115. https://doi.org/10.1016/j.chemosphere.2015.09.045

Sun, J., Quicksall, A. N., Chillrud, S. N., Mailloux, B. J., & Bostick, B. C. (2016). Arsenic mobilization from sediments in microcosms under sulfate reduction. *Chemosphere*, *153*, 254–261. https://doi.org/10.1016/j.chemosphere.2016.02.117

van Geen, A., Bostick, B. C., Thi Kim Trang, P., Lan, V. M., Mai, N.-N., Manh, P. D., et al. (2013). Retardation of arsenic transport through a Pleistocene aquifer. *Nature*, *501*(7466), 204–207. https://doi.org/10.1038/nature12444

Winkel, L. H. E., Trang, P. T. K., Lan, V. M., Stengel, C., Amini, M., Ha, N. T., et al. (2011). Arsenic pollution of groundwater in Vietnam exacerbated by deep aquifer exploitation for more than a century. *Proceedings of the National Academy of Sciences of the United States of America*, *108*(4), 1246–1251. https://doi.org/10.1073/pnas.1011915108

Xie, X., Wang, Y., Su, C., Liu, H., Duan, M., & Xie, Z. (2008). Arsenic mobilization in shallow aquifers of Datong Basin: Hydrochemical and mineralogical evidences. *Journal of Geochemical Exploration*, *98*(3), 107–115. https://doi.org/10.1016/j.gexplo.2008.01.002

Reference From the Supporting Information

Viet, P. H., Tuan, V. V., Hoai, P. M., Anh, N. T. K., & Yen, P. T. (2001). Chemical composition and acidity of precipitation: A monitoring program in Northeastern Vietnam. *Water, Air, and Soil Pollution*, *130*(1–4 III), 1499–1504. https://doi.org/10.1023/A:1013989703593